

ZnGeP₂ optical parametric oscillator with 3.8–12.4- μm tunability

K. L. Vodopyanov, F. Ganikhanov, J. P. Maffetone, I. Zwieback, and W. Ruderman

Inrad, Inc., 181 Legrand Avenue, Northvale, New Jersey 07647

Received February 11, 2000

A ZnGeP₂ (ZGP) optical parametric oscillator (OPO) with wide mid-IR tunability has been demonstrated. The singly resonant angle-tuned ZGP OPO was pumped by 100-ns erbium laser pulses at $\lambda = 2.93 \mu\text{m}$ and yielded output that was continuously tunable from 3.8 to 12.4 μm (type I phase matching) and from 4 to 10 μm (type II phase matching). An OPO pump threshold was less than 1 mJ in the whole 4–12 μm range of the output, and the quantum conversion efficiency reached 35%. An OPO linewidth was typically a few wave numbers; however, with a single intracavity etalon (uncoated Si plate) in a type II OPO it was narrowed to $<0.5 \text{ cm}^{-1}$. We demonstrate the sensitive detection of N₂O gas with the narrow-linewidth OPO. © 2000 Optical Society of America

OCIS codes: 190.2620, 190.4360, 190.4410, 190.4970, 160.4330.

The very high nonlinear-optical coefficient of ZnGeP₂ (ZGP; $d_{\text{eff}} = 75 \text{ pm/V}$), combined with good optical, mechanical, and thermal properties, favors a variety of nonlinear-optical applications, including efficient high-average-power ($>10\text{-W}$) optical parametric oscillators^{1,2} (OPO's) and picosecond–femtosecond optical parametric generators^{3–5} that deliver $>1\text{-MW}$ peak-power pulses. When ZGP-based OPO's are pumped by nanosecond pulses, their infrared tunability is reportedly 6.9–9.9 μm (2.8- μm pump)⁶ and 2.7–8 μm (2.1- μm pump).⁷

We demonstrate in this Letter that the continuous tunability of the ZGP OPO can be extended to the 3.8–12.4- μm range; the long-wave limit of this span is set entirely by the linear transmission of the crystal. We also show that the OPO linewidth can be dramatically reduced without sacrificing much of the conversion efficiency and that such an OPO can be used for sensitive detection of gas.

The pump laser was based on a flash-lamp-pumped Er,Cr,Tm:YSGG crystal ($\lambda = 2.93 \mu\text{m}$). The laser was Q switched by Brewster-cut electro-optical LiNbO₃ and delivered 100–110-ns TEM₀₀ pulses with a linewidth of 0.3 cm^{-1} , a repetition rate of 10 Hz, and an energy of 10 mJ.

ZGP crystals, grown at Inrad, Inc., by the horizontal gradient freeze technique, were 20 mm long (7 mm \times 10 mm cross section) and cut at $\theta_0 = 49.5^\circ$, $\varphi = 90^\circ$ (type I) and $\theta_0 = 70^\circ$, $\varphi = 45^\circ$ (type II). The reflection per face in the 2.93–5.8- μm (i.e., for pump plus signal) range was less than 2%.

An optical damage test of ZGP at $\lambda = 2.93 \mu\text{m}$ $\tau = 100 \text{ ns}$ (exposure, 2000 pulses) has shown that surface damage starts (at both the front and the back surfaces) at a fluence of 3.5 J/cm^2 (35 MW/cm^2); however, no damage was observed for OPO mirrors at a fluence of 3.77 J/cm^2 .

The lowest OPO threshold was obtained in scheme A of Fig. 1 (flat–flat OPO configuration, $L = 2.7 \text{ cm}$). The front mirror, M1, is transmissive ($>75\%$) for the pump and the idler waves and highly reflective (98%) for the signal. A gold rear mirror, M2, highly reflects ($R > 98\%$) pump, signal, and idler. The signal wave

resonates, while the pump and the idler are recycled to have a second pass before leaving the OPO cavity. A dichroic beam splitter (BS) separates the incoming pump beam from the outgoing idler. The pump

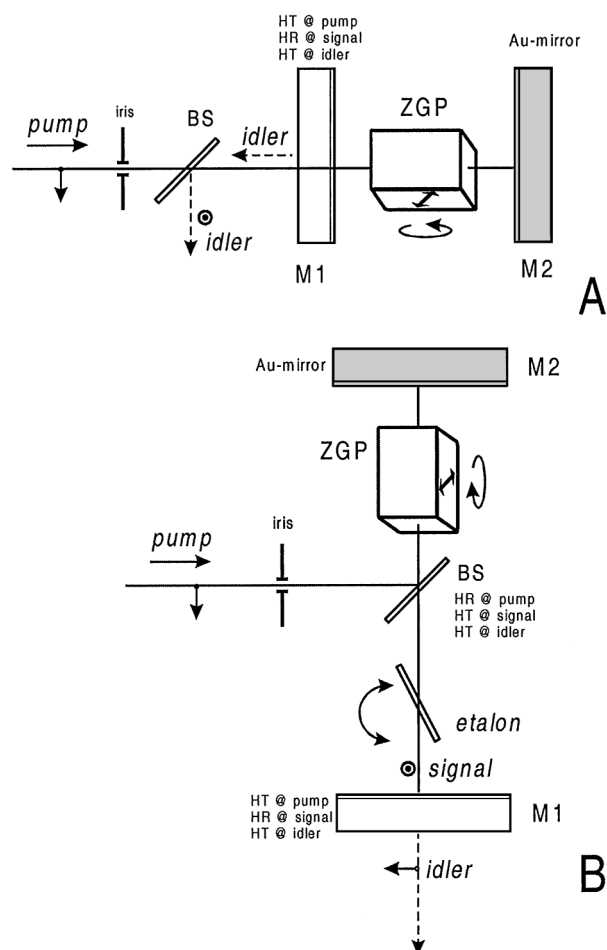


Fig. 1. A, Simple flat–flat OPO configuration ($L = 2.7 \text{ cm}$) with a resonating signal and recycling of pump and idler beams. B, OPO configuration with an intracavity etalon for line narrowing. HT, highly transmissive; HR, highly reflective.

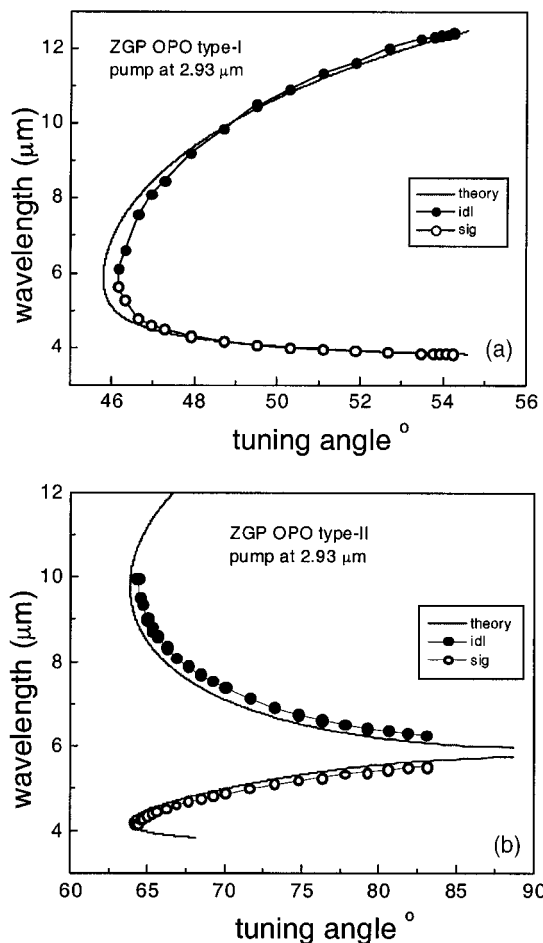


Fig. 2. ZGP OPO angular tuning curves with a $\lambda = 2.93 \mu\text{m}$ pump. (a) Type I OPO; continuous tunability of $3.8\text{--}12.4 \mu\text{m}$ is achieved with a single-orientation crystal. (b) Type II OPO. Solid curves, theoretical, based on dispersion relations.⁸

beam radius ($1/e^2$) was 0.82 mm , and the OPO mirrors were slightly ($\sim 0.25^\circ$) tilted from the normal to the laser beam to prevent laser cavity feedback.

Figure 2(a) shows the ZGP OPO type I angular tuning curve. The solid curve is theoretical, based on the most recent refractive-index measurements.⁸ Continuous tunability (signal plus idler) of $3.9\text{--}12.4 \mu\text{m}$ was achieved with a single-orientation ZGP crystal and a set of two OPO mirrors M1. This is a remarkable range for this crystal; the longest ZGP OPO wavelength previously achieved had been $9.9 \mu\text{m}$.⁶ The OPO linewidth was 5.5 cm^{-1} at $\lambda_{\text{idler}} \approx 10 \mu\text{m}$, 6.5 cm^{-1} near $8 \mu\text{m}$, and rather broader, $20\text{--}30 \text{ cm}^{-1}$, near the degeneracy point ($\sim 6 \mu\text{m}$).

Type II angular tuning curves [Fig. 2(b)] were taken with a similar layout. Continuous tunability of $4\text{--}10 \mu\text{m}$ (with the exception of a small gap at $5.8\text{--}6.1 \mu\text{m}$ near degeneracy) was achieved with a single-orientation ZGP crystal and set of two dichroic OPO mirrors M1. Type II OPO output linewidths are intrinsically narrower than in type I (we obtained 1.5 cm^{-1} at $\lambda_{\text{idler}} = 6.3 \mu\text{m}$ and 2.6 cm^{-1} at $7.7 \mu\text{m}$), and the linewidth decreases (owing to the shape of the type II tuning curve) as the degeneracy point is approached.

Figure 3 shows the dependence of the type I OPO idler beam energy (in the case of type II we got quite similar results) as a function of pump energy for $\lambda_{\text{idler}} = 6.6 \mu\text{m}$ and $\lambda_{\text{idler}} = 8.1 \mu\text{m}$. At $\lambda_{\text{idler}} = 6.6 \mu\text{m}$ the maximum absolute laser-to-idler conversion efficiency was achieved at $\sim 2.4\text{-mJ}$ pump energy (approximately six thresholds) and reached 14.7% , corresponding to a quantum conversion efficiency (signal plus idler) of 33% (Table 1). The maximum idler energy was 1.2 mJ .

At $\lambda_{\text{idler}} = 8.1 \mu\text{m}$ the laser-to-idler conversion efficiency was 12.8% at $1\text{--}2 \text{ mJ}$ pump (approximately four thresholds). This corresponds to a quantum conversion efficiency of 35.3% and a slope efficiency of 41.75% . If we take into account that input OPO mirror M1 transmits only 77% of the pump, we get an even higher value of 54.2% for the quantum slope efficiency.

In configuration A, threshold pump energies (both type I and type II) were as low as $\sim 0.37 \text{ mJ}$, corresponding to a threshold fluence of 0.035 J/cm^2 (0.3-MW/cm^2 intensity), close to the theoretical value (0.02 J/cm^2).⁹ Also, this threshold fluence is 100 times smaller than the ZGP surface damage threshold.

The OPO type I idler energy is plotted in Fig. 4 as a function of the wavelength. The two curves correspond to pump laser energies of 5 and 10 mJ . Also shown (dashed curve) is the pump threshold energy as a function of the idler wavelength. These

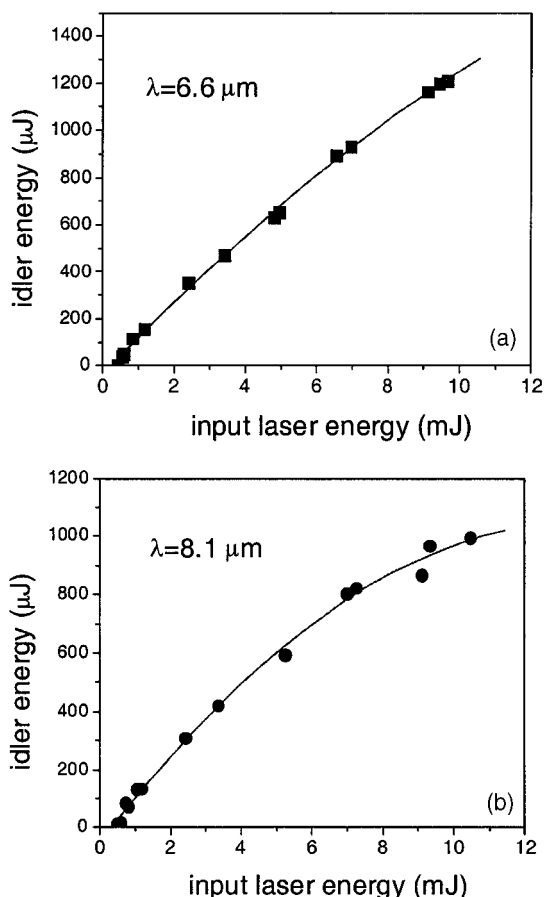


Fig. 3. OPO idler wave energy curves: (a) $\lambda_{\text{idler}} = 6.6 \mu\text{m}$, (b) $\lambda_{\text{idler}} = 8.1 \mu\text{m}$.

Table 1. OPO Output Idler Characteristics As a Function of Wavelength

Wavelength (μm)	Threshold Energy (mJ)	Threshold Fluence (J/cm^2)	Threshold Intensity (MW/cm^2)	Laser-to-Idler Conversion Efficiency (%)	Quantum Conversion Efficiency (%)	Slope Quantum Conversion Efficiency (%)	Maximum Energy (mJ)
6.6	0.37	0.035	0.30	14.7	33	34.3	1.2
8.1	0.4	0.038	0.32	12.8	35.3	41.75	1

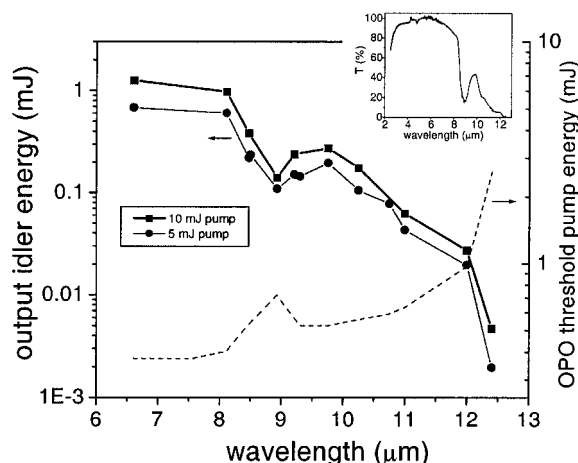


Fig. 4. OPO output as a function of λ_{idler} for two pump energies: 5 and 10 mJ. Dashed curve, the OPO pump threshold dependence. Inset, transmission spectrum of the antireflection-coated $L = 2$ cm ZGP crystal.

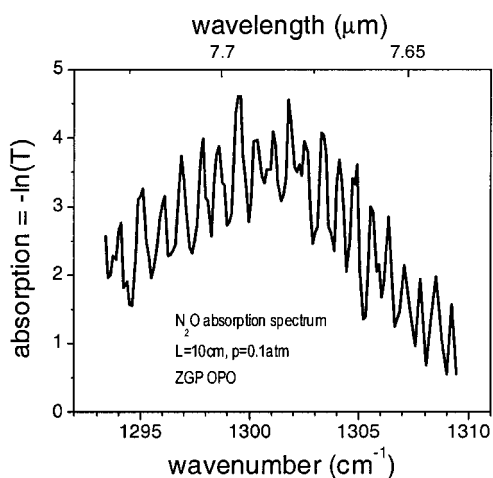


Fig. 5. Absorption spectrum of N_2O gas ($L = 10$ cm, $p = 0.1$ atm) obtained from the OPO transmission experiment.

dependencies correlate with the ZGP transmission spectrum (the inset in Fig. 4 shows transmission of the antireflection-coated $L = 2$ cm ZGP crystal taken with a Perkin-Elmer 1600 FTIR spectrometer). It can also be seen that the pump threshold stays below 1 mJ in the range of 4–12 μm of the OPO output.

The OPO idler beam divergence ($\lambda \approx 8 \mu\text{m}$) was found to be 8.2 mrad in the horizontal and 7.3 mrad in the vertical (kz) planes, which correspond to an approximately $2.5\times$ diffraction limit.

To achieve a narrow linewidth we used a type II OPO, configuration B of Fig. 1, with just one low-

finesse ($F \approx 7$) etalon inside the cavity [we used a tilted (60° – 80°) Si plate, 190 μm thick]. In this way, the OPO linewidth was reduced to less than 0.5 cm^{-1} . The threshold in configuration B was approximately three times higher than that in configuration A, mainly because of the longer OPO cavity ($L = 6$ cm) in configuration A and some etalon losses. The output efficiency decrease was less than 50%, so we observed an overall enhancement of spectral brightness. Smooth OPO wavelength tuning was achieved by simultaneous rotation of the ZGP crystal and the Si plate. The absorption spectrum of N_2O obtained from the transmission experiment is shown in Fig. 5. From the width of the peaks we can estimate the OPO linewidth to be $\sim 0.4 \text{ cm}^{-1}$, in agreement with the previously measured 0.5 cm^{-1} .

The authors acknowledge with appreciation the support of U.S. Air Force Phase I SBIR contract F-40600-97-C-0008. K. L. Vodopyanov's e-mail address is kvodopyanov@inrad.com.

References

1. P. A. Budni, L. A. Pomeranz, M. L. Lemons, P. G. Schunemann, T. M. Pollak, and E. P. Chicklis, in *Advanced Solid-State Lasers*, W. R. Bosenberg and M. M. Fejer, eds. (Optical Society of America, Washington, D.C., 1998), p. 90.
2. E. Cheung, S. Palese, H. Injeyan, C. Hofer, J. Ho, R. Hilyard, H. Komine, J. Berg, and W. Bosenberg, in *Advanced Solid State Lasers*, M. M. Fejer, H. Injeyan, and U. Keller, eds., Vol. 26 of OSA Trends in Optics and Photonics Series (Optical Society of America, Washington, D.C., 1999), p. 514.
3. K. L. Vodopyanov and V. Chazapis, *Opt. Commun.* **135**, 98 (1997); K. L. Vodopyanov, *J. Opt. Soc. Am. B* **16**, 1579 (1999).
4. V. Petrov, Y. Tanaka, and T. Suzuki, *IEEE J. Quantum Electron.* **33**, 1749 (1997).
5. V. Petrov, F. Rotermund, F. Noack, and P. Schunemann, *Opt. Lett.* **24**, 414 (1999).
6. T. H. Allik, S. Chandra, D. M. Rines, P. G. Schunemann, J. A. Hutchinson, and R. Utano, *Opt. Lett.* **22**, 597 (1997).
7. P. B. Phua, K. S. Lai, R. F. Wu, and T. C. Chong, *Opt. Lett.* **23**, 1262 (1998).
8. D. E. Zelmon, E. A. Hanning, and P. Schunemann, "Refractive index measurements and new Sellmeier coefficients of zinc germanium phosphide (ZnGeP_2) from 2–9 microns with implications for phase matching in optical parametric oscillators," *Proc. Mater. Res. Soc. Symp.* (to be published).
9. Obtained from first principles by numerical integration of coupled three-wave equations with Gaussian pump beam intensity distribution in time and in cross section.